Journal of Solid State Chemistry 183 (2010) 1872–1877

Contents lists available at ScienceDirect

Journal of Solid State Chemistry

journal homepage: www.elsevier.com/locate/jssc

Facile synthesis of nanocrystalline wurtzite Cu–In–S by amine-assisted decomposition of precursors

Pulakesh Bera [1], Sang Il Seok*

KRICT-EPFL Global Research Laboratory, Advanced Materials Division, Korea Research Institute of Chemical Technology, 19 Sinseongno, Yuseong, Daejeon 305-600, Republic of Korea

ARTICLE INFO

Article history:
Received 15 January 2010
Received in revised form
15 May 2010
Accepted 14 June 2010
Available online 19 June 2010

Keywords:
Wurtzite copper indium sulfide nanocrystals
Solvothermal process
Precursors

ABSTRACT

Phase-pure ternary wurtzite Cu–In–S nanocrystals have been synthesized by a simple amine-assisted decomposition of mixed precursor complexes derived from S-methyl dithiocarbazate (SMDTC) at a relatively low temperature without using any external surfactant. The crystal phase, morphology, crystal lattice, and chemical composition of the as-prepared products were analyzed by using X-ray diffraction, transmission electron microscopy (TEM), X-ray photoelectron spectroscopy (XPS), and energy-dispersive X-ray spectroscopy (EDX). The optical properties show the pronounced quantum confinement effect in nanocrystals. A possible growth mechanism has been suggested for the formation of anisotropic wurtzite Cu–In–S It is believed that a combined effect of the chelating amine and precursors containing CH_3S unit plays a key role in the formation of the metastable phase of wurtzite Cu–In–S.

1. Introduction

Ternary chalcopyrite semiconductors have received much attention because of their potential applications in photovoltaic cells, light emitting diodes, and non-linear optical devices [1–3]. The ternary chalcopyrite materials made of some restricted elements with general composition $A^{I}B^{III}C_2^{VI}$ favor ionic bonding resembling II–VI type materials [4].

Recently, several types of solar cells are under development to meet energy needs using ternary chalcopyrite [5]. In particular, $CuInS_2$ has been considered greatly as a sensitizer for its high-energy conversion efficiency, high-absorption coefficient ($\sim 10^5\ cm^{-1}$), and less toxicity [6]. The band gap of ternary chalcopyrite semiconductors ranging from 1.5 eV ($CuInS_2$) to 1.1 eV ($CuInSe_2$) is well matched with the solar spectrum. An efficiency of 9–13% of a thin-film solar cell made of $CuInS_2$ has been recorded [7,8]. Generally, $CuInS_2$ exists in three polymorphic forms at different temperatures e.g., chalcopyrite ($>980\ ^\circ C$), zinc blende (980–1050 °C), and wurtzite ($<1050\ ^\circ C$ up to melting point) [9]. The high temperature phases (zinc-blende and wurtzite) are metastable and transform into thermodynamic stable chalcopyrite form at room temperature. High temperature metastable $CuInS_2$ nanoparticles can be obtained at ambient temperature if the particles are properly passivated in the process of synthesis [10]. In literature, several methods have been reported to synthesize colloidal $CuInS_2$ that included solvothermal method [11–14], precursor decomposition method [15–19], and hot injection techniques [20,21]. Among these processes, the precursor decomposition method in suitable solvent and/or surfactant is usually regarded, as it offers the potential advantages of mildness, safety, and simplification of synthetic procedure [22–24]. The potential use of some thio- and selenocarboxylates as single-source precursors for making metal sulfide and selenide thin film and nanoparticle is documented by Vittal and Ng [25] Almost all of the literature methods describe the synthesis of zinc-blende $CuInS_2$ whereas methods for the preparation of wurtzite $CuInS_2$ are practically rare. Observation on wurtzite Cu–In–S proves that the metastable phase is kinetically accessible under less energy-intensive condition. The wurtzite phase shows flexibility in stoichiometry due to different occupancy of the copper and indium atoms in the lattice sites. For this special structural characteristic, the band gap of wurtzite phase of ternary $CuInS_2$ can be tuned over a wide range of energy, which is an essential requirement to fabricate optoelectronics devices.

Very recently in a greener approach, Xie et al. [26] synthesized high quality $CuInS_2$ nanocrystals in the size range from 2 to 20 nm by adjusting the relative amount of Cu-source with In-precursor. Nose et al. [27] currently reported the preparation of different phases of ternary $CuInS_2$ by controlling the ligand species of the metallic monomers. Dialkyl dichalcogenides are used as

* Corresponding author. Fax: +82 42 861 4151.
E-mail address: seoksi@krict.re.kr (S. Il Seok).
[1] Present address: Postgraduate Department of Chemistry, Panskura Banamali College (Vidyasagar University), Midnapore East, West Bengal 721152, India.

0022-4596/$ - see front matter © 2010 Elsevier Inc. All rights reserved.
doi:10.1016/j.jssc.2010.06.006

chalcogenide sources at low temperature to synthesize nanocrystalline wurtzite Cu–In–S in coordinating solvent [28]. In a current article, hexagonal nanostructured wurtzite $CuInS_2$ samples with edge lengths of >100 nm were prepared from stoichiometric amounts of $CuCl_2 \cdot 2H_2O$, $InCl_3 \cdot 4H_2O$, and 20% molar excess thiourea using ethanolamine as capping agent in a solvothermal method [6]. In a very recent article, the epitaxial overgrowth of wurtzite $CuInS_2$ nanorods onto one face of hexagonal Cu_2S nanodisks resulting biphasic Cu_2S–$CuInS_2$ and finally phase transformation of biphase Cu_2S–$CuInS_2$ to wurtzite $CuInS_2$ was reported using a solvothermal synthetic method [12]. Pan et al. [20] reported the synthesis of both zinc blende and wurtzite $CuInS_2$ using mixed precursors $Cu(dedc)_2$ and $In(dedc)_3$ (dedc is diethyl dithiocarbamate) in oleic acid and dodecanthiol as the capping agent, respectively. Solvothermal syntheses of both wurtzite and zinc blende phases of Cu–In–S nanocrystals have been reported using single and dual-source precursors [29]. Despite these recent reports the synthesis of nanostructured wurtzite $CuInS_2$ stably at a room temperature is still a formidable challenge to the synthetic chemists. We herein report a rational synthesis of metastable wurtzite $CuInS_2$ using mixed precursors of $[Cu(SMDTC)Cl_2]$ and $[In(SMDTC)_2Cl_2]$ in common coordinating solvents such as ethylenediamine (EN) and hexamethylenediamine (HMDA). The use of SMDTC derived copper and indium precursors are used for the first time.

2. Materials and methods

2.1. Materials

All reagents used in the present work were of analytical purity and were purchased from Aldrich-Sigma Company. All chemicals were used without further purification.

2.2. Synthesis of precursors

The ligand, S-methyl dithiocarbazate, SMDTC, was obtained by the literature method described earlier [30]. The complex with empirical formula $Cu(SMDTC)Cl_2$ was synthesized by mixing ice-cold ethanolic solution of $CuCl_2 \cdot 2H_2O$ and SMDTC in 1:1 molar ratio with constant stirring. The parrot green compound obtained was filtered, washed with ethanol, and dried over silica gel. For the synthesis of $[In(SMDTC)_2Cl_2]Cl$, a methalonic solution containing $InCl_3$ (98%) and SMDTC in 1:3 molar ratio was refluxed for 2 h. A white product was obtained by evaporating the reaction solvent followed by the addition of $CHCl_3$. The product was filtered and washed with a mixture of $CHCl_3$ and MeOH (v/v 5:1), and dried over silica gel. Yield for $Cu(SMDTC)Cl_2$: 70%. $\Lambda_m = 23\ \Omega^{-1}\ cm^{-2}\ mol^{-1}$, Anal. Calc. for $C_2H_6N_2S_2CuCl_2$: C, 9.35; H, 2.33; N, 10.91; and S, 24.95. Found: C, 9.91; H, 2.41; N, 10.78; and S, 25.80%. IR frequencies in cm^{-1} (assignments): 3114.4 ($\nu_{NH/NH2}$), 1596.6 ($\nu_{C-N\ \&\ N-N}$), 1497 (ν_{C-N}), 1380.9 (ν_{N-N-C}), and 984 ($\nu_{C=S}$). Yield for $[In(SMDTC)_2Cl_2]Cl$: 75%. $\Lambda_m = 110\ \Omega^{-1}\ cm^{-2}\ mol^{-1}$, Anal. Calc. for $C_4H_{12}N_4S_4InCl_3$: C, 10.31; H, 2.57; N, 12.03; and S, 27.51. Found: C, 10.20; H, 2.50; N, 13.75; and S, 27.31%. IR frequencies in cm^{-1} (assignments): 3126.55 ($\nu_{NH/NH2}$), 1608.44 ($\nu_{C-N\ \&\ N-N}$), 1498.86 (ν_{C-N}), 1424.28 (ν_{N-N-C}), and 997.78 ($\nu_{C=S}$).

2.3. Synthesis of $CuInS_2$ nanoparticles

In a typical synthesis, an intimate mixture of as-prepared $[Cu(SMDTC)Cl_2]$ (0.128 g, 0.5 mmol) and $[In(SMDTC)_2Cl_2]Cl$ (0.232 g, 0.5 mmol) was taken with 10 ml of EN in a 50 mL two-necked flask equipped with a condenser and thermocouple adaptor. The flask was degassed at room temperature for 10 min and then filled with argon gas. The resultant solution was then gradually heated up to 120 °C and was maintained at this temperature for 1 h under an argon atmosphere by which time a black suspension was formed. The black precipitate was collected by centrifugation and then the isolated solid was dispersed in ethanol. The nanoparticles (NPs) were initially purified by dispersing the particles with excess ethanol and discarding the supernatant after centrifugation. The above centrifugation and isolation procedure was repeated 4–5 times with aqueous ethanol (75%) for the purification of the product and dispersed again in ethanol for further characterization. The powder was dried at 90 °C for 1 h. The reaction conditions were varied to investigate the effect of different reaction parameters on the size and morphology of the product. The same experimental procedure was repeated with Cu/In ratio 1:2 to observe the effect of stoichiometric ratio of the used precursors. Two additional experiments were carried out in HMDA, a longer chelating diamine than EN, at two different temperatures (180–200 °C) to examine the effect of solvent following the above synthetic procedure.

2.4. Characterization techniques

The elemental analysis (C, H, N, and S) of the complex was performed using FISONS EA-1108 CHN analyzer. The IR spectra (4000–500 cm^{-1}) were recorded on a Bruker EQUINOX 55 FT-IR spectrophotometer. The TG analysis was carried out on a TGA Q500 V6.7 Build 203 TG instrument at a heating rate of 10 °C/min under nitrogen. UV–visible absorption spectra were recorded on a Shimadzu UV 2550 spectrophotometer in 200–800 nm wavelength range at room temperature. TEM of copper sulfide NPs was characterized using a FEI Tecnai G^2 T-20S at an accelerating voltage of 200 kV. The TEM samples were prepared by placing a drop of a dilute ethanol dispersion of NPs on the surface of a 200-mesh carbon-coated copper or nickel grid. The EDAX plots were obtained using the AMETEK Energy Dispersive Analysis System operating at 200 kV at a tilt angle of 15°. Powder X-ray diffraction (XRD) was recorded using a Rigaku D/2200 V diffractometer. Measurements were taken using graphite-monochromated Cu$K\alpha$ radiation ($\lambda = 1.5418$ Å) with a scan rate of 5°/min over a range of $5^\circ < 2\theta < 80^\circ$ with steps of 0.02° and scintillation detector is operating at 40 kV and 40 mA. XPS was performed on an AXIS NOVA X-ray photoelectron spectroscopy, using monochromatised Al$K\alpha$ radiation with an anode voltage of 15 kV and emission current of 10 mA, the low resolution survey spectrum was recorded with a pass energy of 160 eV, high resolution spectrum was recorded with a pass energy of 20 eV, and the quantification was calculated by area calculation.

3. Results and discussion

The air-stable precursors are easily synthesized under atmospheric bench-top conditions and the as-synthesized precursors were used without further purification for the preparation of wurtzite $CuInS_2$, which meets the goal of environmentally friendly synthesis and low cost materials. The precursor complexes were characterized by means of elemental analysis (C, H, N, and S), FTIR, conductance measurements (see experimental section), and thermogravimetry analysis (TGA). SMDTC molecule acts as a bidentate ligand co-coordinating through the thiol S-atom and the terminal hydrazinic N atom to the metal atom as evidenced by the shifting of $\nu_{NH/NH2}$ frequencies in IR spectrum appearing in the range 3300–3175 cm^{-1} in the free-ligand spectrum to the lower frequency region in the complexes

(3113 and 3126 cm^{-1} for copper and indium, respectively) and the vibration bands at 984 cm^{-1} for Cu-complex and 997 cm^{-1} for In-complex due to C=S stretching vibrations shift to high energy by 43–56 cm^{-1} in comparison with free ligand pointing to the participation of the sulfur atom of the C=S group as a possible coordination site [31]. The proposed structures of the precursors are given in Fig. 1. TGA of the precursors is recorded to study the thermal behavior and suitability for the preparation of $CuInS_2$. The decomposition of $Cu(SMDTC)Cl_2$ starts at ca. 100 °C as shown in Fig. 1a. This complex precursor undergoes a significant weight loss of 63.15% (calculated 62.74%) in the first stage due to the combined loss of Cl_2 and $MeSCNHNH_2$ unit of ligand giving a residue, which is close to the value calculated for the mass percentage of bulk CuS (37.25%). Further insignificant weight loss may be attributed to the loss of sulfur from the ideal stoichiometry of CuS during phase transformation of copper sulfide leading to the formation of copper rich Cu_xS (where $1<x<2$). Similarly, $[In(SMDTC)_2Cl_2]Cl$ starts to decompose at ~164 °C showing a major weight loss of 34.76% (calcd. 34.58%) due to the combined loss of Cl_2 and $MeSCNHNH_2$ unit of one SMDTC (Fig. 1b). Another significant weight loss of 30.24% (calcd. 33.8%) at ca. 280 °C may be attributed for the combined loss of remaining SMDTC and chloride forming InS. TGA results thus, reveal that the two precursors can be used separately to prepare corresponding metal sulfides particles. The use of mixture of these two precursors with different decomposition temperatures is quite judicious to synthesis of $CuInS_2$ in a solvothermal method where early decomposition of $Cu(SMDTC)Cl_2$ with respect to $[In(SMDTC)_2Cl_2]Cl$ is required to give Cu_2S nanostructure template for the growth of wurtzite Cu–In–S as proposed in our formation mechanism. In our experiments, the reaction temperature is chosen to be higher than that of the decomposition temperature of $[In(SMDTC)_2Cl_2]Cl$ (164 °C) so that both the precursors can be decomposed completely. Below this temperature, amines like HMDA, hexylamine, octylamine, etc. are unsuitable for the synthesis of ternary chalcopyrite from the mixture of precursors where the binary hexagonal Cu_2S is the only product as revealed by the XRD (Fig. S1). But EN furnishes nanocrystalline $CuInS_2$ near its boiling temperature, which reveals that EN acts as a very good attacking agent depleting the stability of both the precursors in reaction conditions. Additionally, we also examine the effect of non-chelating monoamines such as hexylamine (b.p. 133 °C) and octylamine (b.p. 178 °C) to synthesise ternary Cu–In–S at their boiling point keeping the other synthetic conditions unchanged. The expected wurtzite Cu–In–S is obtained from octylamine (180 °C, 1 h) whereas hexylamine (130 °C, 1 h) produces binary copper sulfide as ascertained by the XRD of the obtained product (Fig. S2). From these experimental results, it can be safely concluded that both diamine and monoamines can be used as solvents for the synthesis of wurtzite $CuInS_2$ beyond the decomposition temperature of $[In(SMDTC)_2Cl_2]Cl$ i.e., 164 °C, where both precursors are expected to form intermediate complexes with amines breaking the primary coordination sphere. But small chelating EN has some unique capability to produce Cu–In–S at relatively low temperature with respect to HMDA. The reason may be due to the formation of less sterically hindered intermediate complex core with five-membered chelate rings than the nine-membered chelate intermediate in case of HMDA, and as a consequence the metal in less sterically encumbered complex is quite exposed to the incoming ions for further reaction.

In ternary system, three elements are involved in the reaction and there is a high chance to form heterostructure rather than single molecular structure if the activities of the metal precursors are different [32]. The co-decomposition of our mixed precursors having similar bonding properties with SMDTC (neutral NS bidentate) is a successful synthetic procedure for the single phase Cu–In–S. The formation of single phase Cu–In–S in various amines reveals that the nucleation and growth processes are well separated in the solvothermal process. In our method, the product is only the metastable form of wurtzite Cu–In–S in various amines specially diamines, which indicates that the precursors derived from SMDTC having some novelty. The presence of SCH_3 group in its structure may make it to be a promising candidate with the expectation that the in situ generated CH_3S^- ion will stabilize the nanoparticles [14] and also prevent any unwanted oxidation by circumfusing the seeded nanoparticles [33]. It is also believed that in nucleation stage, the nucleus is capped first internally by the short chain CH_3SH whatever the capping agents present in the reaction. So, it can be reasonably expected that the alkyl thiol group in the ligand molecule with similar bonding properties to Cu and In play a key role in the formation of single phase of ternary Cu–In–S. In addition to this, the solvents also play important role in the anisotropic growth of nanocrystals. The bidendate chelating solvents serve the purpose of shape-directing agent and reducing agent simultaneously. It reduces Cu(II) ion to its monovalent oxidation state at reaction temperature.

The phase and crystallinity of the prepared samples were investigated by X-ray diffraction (XRD), as shown in Fig. 2. It is interesting to note that the diffraction patterns can be indexed to hexagonal wurtzite phase of Cu–In–S with clear appearance of characteristic (1 0 0), (0 0 2), (1 0 1), (1 0 2), (1 1 0), (1 0 3), (1 1 2),

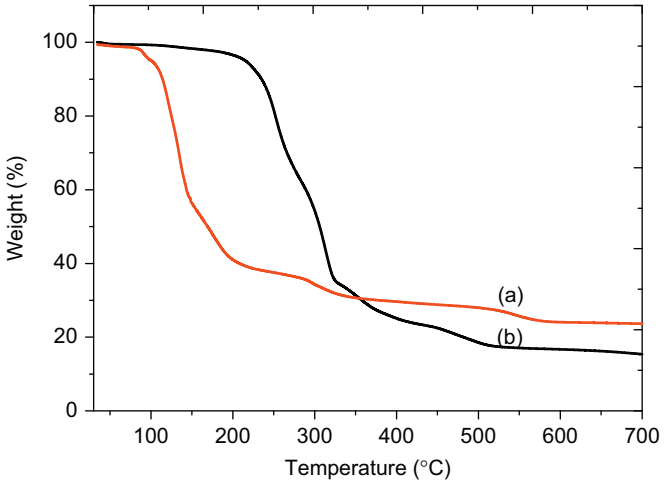

Fig. 1. TGA plots for the decomposition of (a) $Cu(SMDTC)Cl_2$ and (b) $[In(SMDTC)_2Cl_2]Cl$ under nitrogen atmosphere.

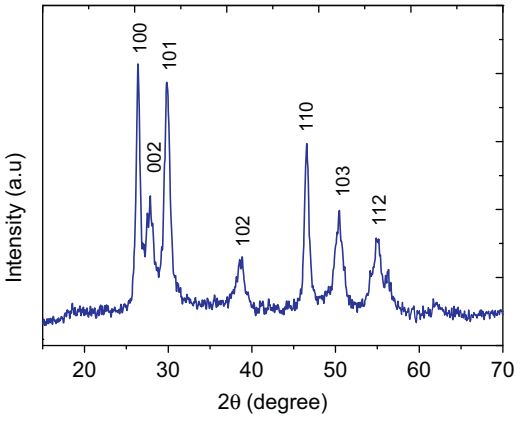

Fig. 2. XRD pattern of $CuInS_2$ nanocrystals obtained in hexamethylene diamine at 180 °C (1 h).

and (2 0 2) peaks. The patterns of the prepared Cu–In–S are well matched with those of reported wurtzite $CuInS_2$ in the literature [6,26,28,29]. The strong and sharp diffraction peak for the (1 0 0) spacing of the hexagonal plane suggests that the crystalline domains are extended along *a*-axis, and the broad diffraction for the (1 0 3) spacing, which has a major contribution for the *c*-axis, suggests a short *c*-axis. The suppression of *c*-axis and elongation along *a*-axis appropriately results in anisotropic crystal structures. Accordingly, the mean 'width', *d*, of the nanocrystals was derived from the (1 0 3) peak ($2\theta = 50.3^\circ$). The mean size of the nanocrystals calculated from the XRD results using Scherrer formula is found to be 15.5 nm for the sample obtained from EN with Cu/In precursor ratio 1, which is consistent with the value observed by TEM.

The morphology and the crystal structure of the sample were further examined by TEM (HRTEM), and selected area electron diffraction (SAED). The TEM (HRTEM) images of the nanocrystals obtained at different reaction conditions are shown in Fig. 3. Fig. 3a shows the anisotropic hexagonal nanoplates obtained from EN with edge lengths of 55(0.5)–66(0.5) nm and widths of 16(0.2)–22.5(0.2) nm. The incomplete edge is the common feature of the elongated hexagonal rods. A magnified view of the edge of nanoplate (Fig. 3b) clearly indicates the presence of the lattice fringes with spacing about 6.43 Å, which is in good agreement with the interplanar spacing of (1 0 0) planes of wurtzite $CuInS_2$ [6]. The corresponding SAED pattern (Fig. 3c) shows well-crystallized single crystal nature of the product with expected six-fold symmetry for wurtzite $CuInS_2$. The sample shows polydispersity as the surface passivation of nanocrystals are met by solvent molecules lonely which are not so copious surfactants like long chain organics. As the [Cu]/[In] precursor ratio changed from 1 to 0.5, some hexagonal platelets have been observed in the colloidal product (Fig. 3d). HRTEM image of a single hexagonal nanostructure was shown in Fig. 3e. The average diameter of the nanoplates is approximately 65 nm with the aspect ratio ~2. A magnified view of the edge of nanoplate (Fig. 3f) clearly demonstrates the presence of the lattice fringes with spacing of 3.33 Å corresponding to (0 0 2) plane of hexagonal wurtzite $CuInS_2$. It is important to note that the variation in [Cu]/[In] precursors ratio in the synthesis produces nanocrystals with same hexagonal morphologies but different aspect ratio. Fig. 3g shows the TEM of the obtained $CuInS_2$ using HMDA at 180 °C (1 h), which clearly demonstrates the rod morphology with lengths in the range of 30–32 nm and widths in the range of 8–9 nm and the clear crystallinity observed in a single nanorod's HRTEM (inset, Fig. 3g) with lattice fringe spacing 3.33 Å corresponds to the (0 0 2) plane of hexagonal $CuInS_2$. As the reaction time is prolonged to 2 h for the synthesis of $CuInS_2$ using HMDA at 200 °C, the morphology of the nanoparticles appears as spherical (Fig. 3h) with hexagonal faceted structure (dashed line, inset, Fig. 3h); '*d*' spacing 3.33 Å indexing the wurtzite $CuInS_2$.

The compositions of $CuInS_2$ and valence state of the constituent metal atoms were investigated by XPS as shown in Fig. 4. The binding energy values in the high-resolution core level spectra of Cu 2p, In 3d, and S 2p are well matched with the reported values [6,14,20]. The Cu 2p signal reaches its maximum value at a binding energy (BE) of 929.9 eV with a split orbit of 20 eV without shake up satellites due to the presence of Cu(+1) in the sample [34]. Another close up survey in the S 2p region (160.4 eV) shows the presence of doublet peaks with an energy difference of 1 eV (Fig. 4c) that can be assigned to sulfur coordinated to Cu and In [35]. The quantification report of XPS (see Table S1) shows that the sample is composed of copper, indium, and sulfur with atomic ratio 1.68:1:1.94, which reveals that the sample is copper rich with respect to the stoichiometry $CuInS_2$. The selected-area energy-dispersive X-ray spectroscopy (EDX) analysis (Cu, In, S) of the products obtained from EN using different [Cu]/[In] precursors ratio 1 and 0.5 and in HMDA at 200 °C using [Cu]/[In] precursors ratio 1 (Fig. S3) confirmed the presence of elements Cu, In, and S. But the samples were found to be compositionally copper rich. The copper-rich composition of $CuInS_2$ seems at odds with the XRD data, which confirms phase-pure hexagonal $CuInS_2$. However, it can be explained by assuming the difficulty in incorporating of larger indium atoms into the crystal structure [20] and the use of copper grid in sampling may be the other possible reason for high value of copper in samples.

The room temperature UV–vis absorption spectra (Fig. 5) of the Cu–In–S revealed that the nanocrystals absorb in the visible wavelength region, indicating a potential solar energy absorber. The absorption spectra of the nanocrystals show a broad absorption peak in the range 430–450 nm with a trail in the lower energy direction. There are no pronounced excitonic peaks

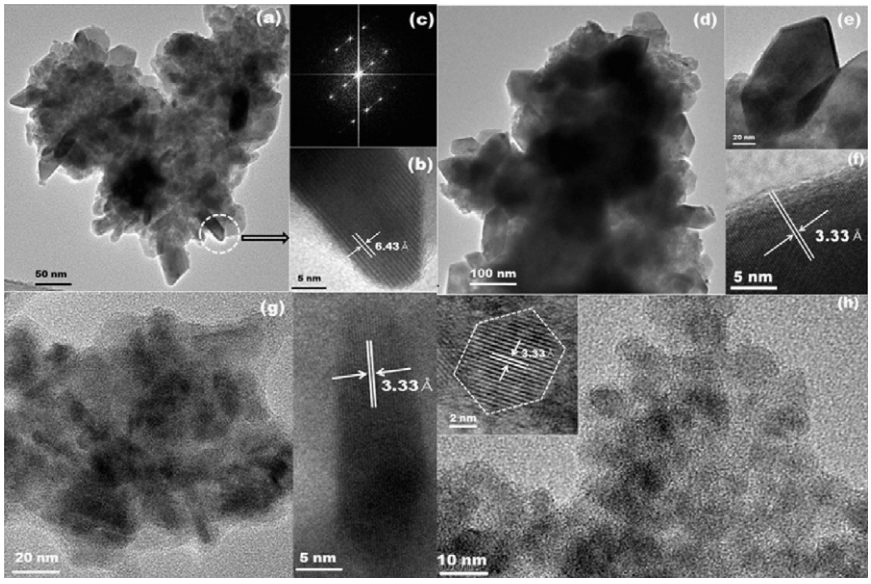

Fig. 3. TEM images of the $CuInS_2$ nanocrystals obtained by thermolysis of mixed precursors in ethylenediamine (117 °C, 1 h) with Cu/In precursor ratio 1 (a–c) and with Cu/In precursor ratio 0.5 (d–f), and in hexamethylenediamine with Cu/In precursor ratio 1 at 180 °C for 1 h (g), and at 200 °C for 2 h (h).

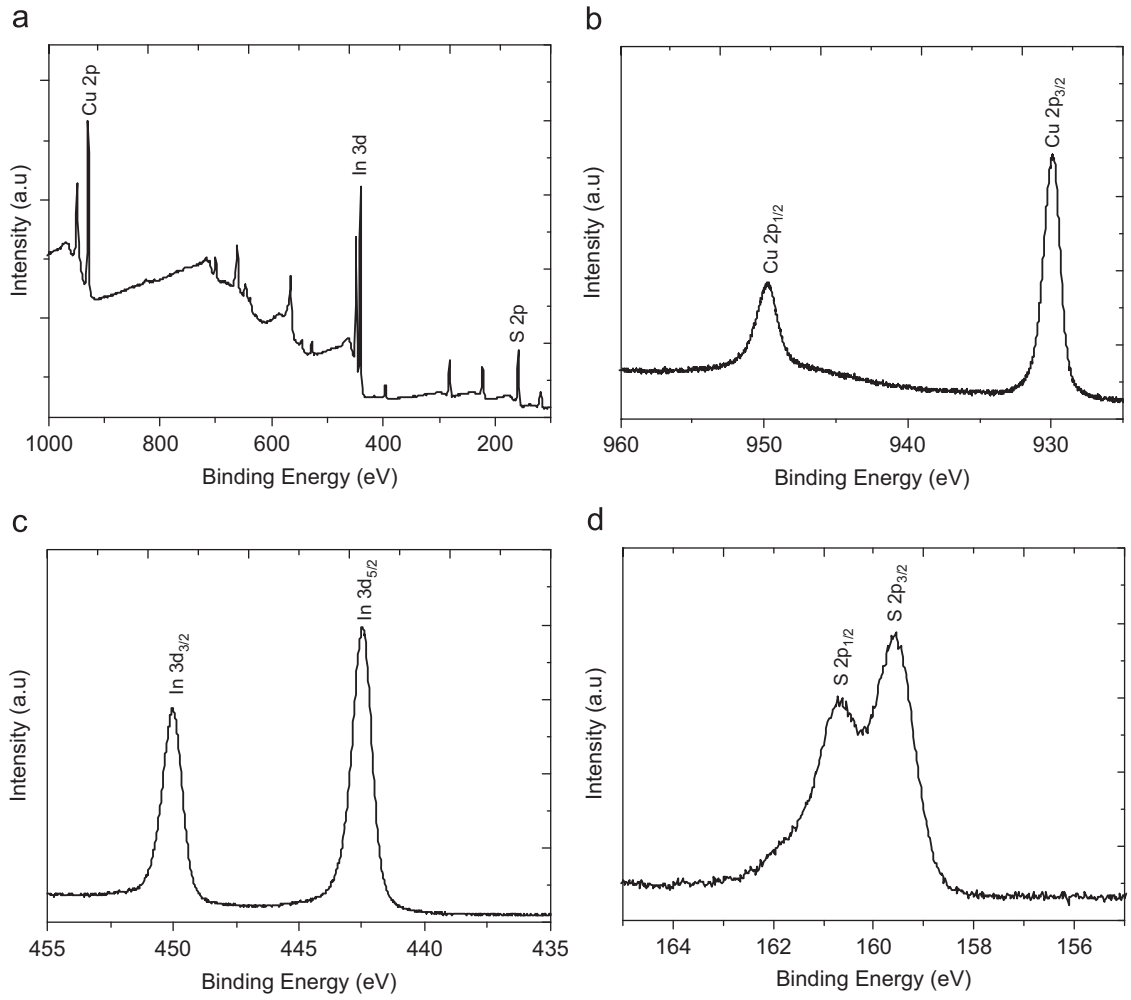

Fig. 4. XPS spectra of wurtzite $CuInS_2$ obtained in hexamethylene diamine at 180 °C (1 h) with Cu/In precursor ratio 1. Survey spectrum (a), high-resolution spectrum of Cu 2p (b), In 3d (c), and S 2p (d).

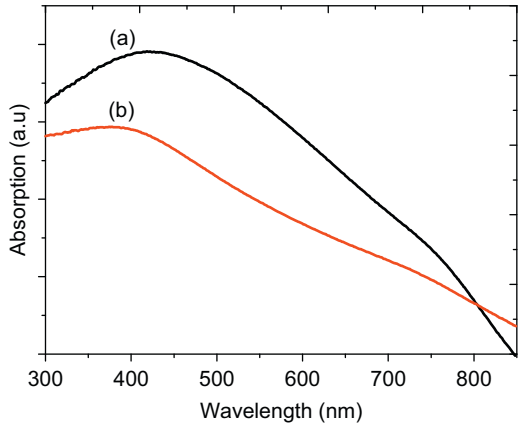

Fig. 5. Absorption spectra of $CuInS_2$ nanocrystals in ethanol obtained by thermolysis of mixed precursors with Cu/In molar ratio 1 in (a) ethylenediamine at 117 °C (1 h) and (b) hexamethylene diamine at 180 °C (1 h).

in the wave range from 600 to 800 nm but a weak shoulder is observed at around $\lambda = 750–760$ nm, which corresponds to 1.78–1.76 eV in energy. The energy 1.78–1.76 eV is greater than the bulk energy band gap of $CuInS_2$ (1.45 eV) [13]. The higher optical band gap of the prepared nanocrystals is attributed to the quantum size effect.

On the basis of the above analytical evidences, we propose the following mechanism for the formation of anisotropic wurtzite Cu–In–S nanocrystal. The initial step is the decomposition of Cu-precursor in presence of chelating solvent followed by the nucleation of hexagonal chalcocite (Cu_2S), which are assumed to be capped internally by CH_3SH (a decomposition product). This Cu_2S nucleus with controllable morphology then acts as template for the anisotropic growth of nanocrystals where chelating solvent molecules again bind preferentially the polar facets of hexagonal Cu_2S nucleus leaving the non-polar (1 0 0) facets more exposed for the incoming ions [36]. In the second step, at a relatively higher reaction temperature (> 167 °C), the coordination sphere of In-precursor gets destroyed and produces solvated In^{3+} ions, S^{2-} ions, and other volatile organics in the alkaline reaction condition [37]. The final stage is the kinetically driven proportionate insertion of dissolved In^{3+} and S^{2-} to the exposed (1 0 0) facets of Cu_2S microstructure leading to the subsequent anisotropic growth of hexagonal Cu–In–S nanostructures along *a*-axis. Furthermore, the formation of nearly spherical Cu–In–S using octylamine, a non-chelating monodentate amine, supports the proposed mechanism where both the polar and non-polar facets absorbed monoamines leading to an isotropic growth of nanocrystals. In a recent report, Conner et al. [12] modeled a multi-step formation mechanism of anisotropic wurtzite $CuInS_2$ that entailed the formation of biphasic Cu_2S–$CuInS_2$ through absorption of reactants on only one side of the Cu_2S nanodisks,

which were nucleated at the starting of the reaction and finally a phase transformation of biphasic Cu_2S–$CuInS_2$ into wurtzite $CuInS_2$ nanorods occurred with growth progression. This observation is also supportive to our proposed mechanism. A further exploration is needed to get a more precise formation mechanism of such ternary nanomaterials.

4. Summary

In this study, we have described a rational synthesis of metastable wurtzite Cu–In–S nanomaterials by using mixed-precursors derived from S-methyl dithiocarbazate. A singularity of phases and narrow size distribution of the ternary products were achieved in the amine-assisted synthesis at relatively low temperature. By the careful selection of chelating amine and reaction parameters, the size of the nanomaterials can be tuned in the nanometric range. In addition, by adjusting the reaction conditions, different morphologies such as nanoplates, nanorod, and hexagonal spheres have been obtained. A mechanism for the anisotropic growth of wurtzite $CuInS_2$ has also been described. We attribute that the presence of CH_3S units in thiosemicarbazide in our primary ligand of the precursor complexes along with the chelating property of diamine has combined effect to the formation of anisotropic wurtzite Cu–In–S. Moreover, the nanocrystals demonstrate fair solubility in common solvents, such as ethanol and toluene, which allow their processing through the simple casting or printing process.

Acknowledgments

This work was supported by the Global Research Laboratory (GRL) Program funded by the Ministry of Education, Science, and Technology, and by a Grant from the Fundamental R&D Program for Core Technology of Materials funded by the Ministry of Knowledge Economy, and Republic of Korea.

Appendix A. Supplementary material

Supplementary data associated with this article can be found in the online version at doi:10.1016/j.jssc.2010.06.006.

References

[1] S. Wagner, P.M. Bridenbugh, J. Cryst. Growth 39 (1977) 151.
[2] R.S. Roth, H.S. Parker, W.S. Brower, Mater. Res. Bull. 8 (1973) 333.
[3] S. Cattarin, C. Pagura, L. Armelao, R. Bertoncello, N. Dietz, J. Electrochem. Soc. 142 (1995) 2818.
[4] M. Uehara, K. Watanabe, Y. Tajiri, H. Nakamura, H. Maeda, J. Chem. Phys. 129 (2008) 134709.
[5] X. Tang, J. Qian, Z. Wang, H. Wangb, Q. Feng, G. Liua, J. Colloid Interface Sci. 330 (2009) 386.
[6] Y. Qi, Q. Liu, K. Tang, Z. Liang, Z. Ren, X. Liu, J. Phys. Chem. C 113 (2009) 3939.
[7] J. Klaer, J. Burns, R. Henninnger, K. Siemer, R. Klenk, K. Ellmer, D. Brauning, Semicond. Sci. Technol. 13 (1998) 1456.
[8] J.T. Theresa, M. Meril, K.C. Sudha, K.P. Vijayakumar, T. Abe, Y. Kashiwaba, Sol. Energy Mater. Sol. Cells 89 (2005) 27.
[9] J.J.M. Binsma, L.J. Giling, J. Bloem, J. Cryst. Growth 50 (1980) 429.
[10] Y. Zhao, Y. Zhang, H. Zhu, G.C. Hadjipanayis, J.Q. Xiao, J. Am. Chem. Soc. 126 (2004) 687.
[11] K. Das, D.P. Dutta, S. Chaudhuri, Cryst. Growth Des. (2007) 1547.
[12] S.T. Connor, C.M. Hsu, B.D. Weil, S. Aloni, Y. Cui, J. Am. Chem. Soc. 131 (2009) 4962.
[13] W.M. Du, X.F. Qian, J. Yin, Q. Gong, Chem. Eur. J. 13 (2007) 8840.
[14] H. Zhong, Y. Zhou, M. Ye, Y. He, J. Ye, C. He, C. Yang, Y. Li, Chem. Mater. 20 (2008) 6434.
[15] J.S. Gardner, E. Shurdha, C. Wang, L.D. Lau, R.G. Rodriguez, J.J. Park, J. Nanopart. Res. 10 (2008) 633.
[16] J.J. Nairn, P.J. Schapiro, B. Twamley, T. Pounds, R.V. Wandruszka, M. Williams, C.M. Wang, M.G. Notton, Nano Lett. 6 (2006) 1218.
[17] S.L. Castro, S.G. Bailey, K.K. Banger, A.F. Hepp, J. Phys. Chem. B 108 (2004) 12429.
[18] S.L. Castro, S.G. Bailey, R.P. Raffaelle, K.K. Banger, A.F. Hepp, Chem. Mater. 15 (2003) 3142.
[19] K.K. Banger, M.H.C. Jin, J.D. Harris, A.F. Hepp, Inorg. Chem. 42 (2003) 7713.
[20] D.C. Pan, L.J. An, Z.M. Sun, W. Hou, Y. Yang, Z.Z. Yang, Y.F. Lu, J. Am. Chem. Soc. 130 (2008) 5620.
[21] H. Nakamura, W. Kato, M. Uehara, K. Nose, T. Omata, S.O. Matsuo, M. Miyazaki, H. Maeda, Chem. Mater. 18 (2006) 3330.
[22] D. Fan, M. Afzaal, M.A. Mallik, C.Q. Nguyen, P. O'Brien, P.J. Thomas, Coord. Chem. Rev. 251 (2007) 1878.
[23] N. Pickett, P. O'Brien, Chem. Rec. 1 (2001) 467.
[24] T. Trindade, P. O'Brien, N.L. Pickett, Chem. Mater. 13 (2001) 3843.
[25] J.J. Vittal, M.T. Ng, Acc. Chem. Res. 39 (2006) 869.
[26] R. Xie, M. Rutherford, X. Peng, J. Am. Chem. Soc. 131 (2009) 5691.
[27] K. Nose, Y. Soma, T. Omata, S. Otsuka-Yao-Matsuo, Chem. Mater. 21 (2009) 2607.
[28] M.E. Naroka, M.A. Franzman, R.L. Brutchey, Chem. Mater. 21 (2009) 4299.
[29] S.K. Batabyal, L. Tian, N. Venkatram, J.J. Vittal, J. Phys. Chem. C 113 (2009) 1503.
[30] P. Bera, C.H. Kim, S.I. Seok, Inorg. Chim. Acta 362 (2009) 2603.
[31] P. Bera, C.H. Kim, S.I. Seok, Polyhedron 27 (2008) 3433.
[32] S.H. Choi, E.G. Kim, T. Hyeon, J. Am. Chem. Soc. 128 (2006) 2520.
[33] J. Aldana, Y.A. Wang, X. Peng, J. Am. Chem. Soc. 123 (2001) 8844.
[34] Y.B. Lou, A.C.S. Samia, J. Cowen, K. Banger, X.B. Chen, H. Lee, C. Burda, Phys. Chem. Chem. Phys. 5 (2003) 1091.
[35] J. Shan, P. Pulkkinen, U. Vainio, J. Maijala, J. Merta, H. Liang, R. Serimaa, E. Kauppinen, H. Tenhu, J. Mater. Chem. 18 (2008) 3200.
[36] Y. Li, H. Liao, Y. Ding, Y. Qian, L. Yang, G. Zhou, Chem. Mater. 10 (1998) 2301.
[37] H. Tang, M. Yan, H. Zhang, M. Xia, D. Yang, Mater. Lett. 59 (2005) 1024.